A. SPECIFIC AIMS

The wrist is used in a variety of functions of daily life. Situated between the forearm and the hand, the human carpus is subject to a wide range of injuries and disease both acute and chronic in nature. As one of the most complicated and poorly understood joints in the body, knowledge of carpal kinematics should be beneficial to both basic scientists and clinicians alike. Improving our understanding of carpal kinematics under functional conditions has wide ranging applications including designing ergonomic tools, rehabilitation protocols, and the next generation of total wrist prostheses, which have thus far proven to have a high complication rate.

The majority of our knowledge of carpal kinematics is based on measuring the unloaded wrist in the traditional orthogonal directions of flexion/extension and radial/ulnar deviation. However, it has been hypothesized that a "coupled" wrist motion from radial extension to ulnar flexion is a more physiologic motion. Called the Dart Throwers Motion (DTM), this motion has been shown to play an important role in daily function and is used in a variety of daily activities. Studies have shown that radiocarpal motion is reduced during the DTM, but this has never been confirmed during an actual functional task.

The purpose of our first aim is to measure the *in vivo* 3-D kinematics of the wrist and forearm during a functional task that is purported to use the DTM. We have chosen a simulated hammering task, as hammering is a dominant task of modern man and is an important functional motion. Markerless Bone Registration allows us to study the complex three-dimensional (3-D) motion of the entire carpus *in vivo*, in a non-invasive manner. By studying this motion *in vivo*, our goal is to provide data for the many theories and to allow us to understand the carpal kinematics during this motion.

In addition to passive motion, the wrist is often subject to loading; most commonly during pushing or pulling. All kinematic studies to date on the loading of the wrist have been performed in cadavers or were limited in their measurements. By not studying the wrist under these loaded conditions, our knowledge of carpal kinematics is incomplete. In the second aim, our goal is to measure the *in vivo* effect of loading on the interaction between carpal bones during two tensive or pulling tasks, and one compressive or pushing task.

Specific Aim 1.
To determine the kinematics of the wrist and forearm during simulated hammering. 14 volunteers (7 male, 7 female; age 18-45) with no history of wrist disease will be CT scanned in 5 positions of hammering (2 windup, 1 neutral, 2 impact). 3-D kinematics of the carpus and the DRUJ will be calculated using a markerless bone registration methodology.
Hypothesis 1.1: *Wrist motion follows the DTM during a simulated hammering task.*
Hypothesis 1.2: *During the hamming task, there is zero rotation of the scaphoid or lunate.*

Specific Aim 2.
Measure the change in carpal kinematics during compressive and tensive tasks. The same 14 volunteers from Aim 1, will be scanned performing three tasks (one compressive and two tensive) each without and with resistance (22 lbs or 98 N) for a total of 6 images. The wrist will be positioned in a "push-up" position for the compressive task, gripping a handle for the first tensive task and open in finger traps with the forearm muscles relaxed for the second tensive task. Changes in posture and bone spacing will be measured using a markerless bone registration technique.
Hypothesis 2.1: *Tensive loading of the wrist without gripping causes equal separation at the radiocarpal, midcarpal, and carpal-metacarpal joints.*
Hypothesis 2.2: *Tensive loading of the wrist with active gripping causes no separation at the radiocarpal, midcarpal, or carpal-metacarpal joints.*

Hypothesis 2.3: *The distance between the radius and the proximal row is not altered with compressive loading of the extended wrist.*

B. BACKGROUND AND SIGNIFICANCE

The human carpus is required to perform a wide variety of tasks in modern life. Able to rotate with two principal degrees of freedom and partially a third degree of rotational freedom (Palmer et al. 1985), the wrist has a large range of motion (Li et al. 2005) of which almost 70% is used in most activities of daily life (Ryu et al. 1991). The wrist is heavily involved in essential tasks such as personal hygiene, eating, and opening doors, as well as those of our earlier ancestors such as spear throwing, clubbing and hammering.

The human wrist is the subject of significant injury. Traumatic injuries of the wrist are dominated by bone fracture and ligament tears, both of which have been shown to alter the normal kinematics of the wrist (Short et al. 2002; Crisco et al. 2003; Leventhal et al. 2008). Altered kinematics has been shown to lead to wrist osteoarthritis (Watson et al. 1984). Chronic injuries such as Kienbock's disease have also been shown to alter the normal kinematics of the wrist (Iwasaki et al. 1998) and are known to progress to osteoarthritis with debilitating results (Schuind et al. 2008).

Our limited understanding of wrist function has resulted in few choices for patients with advanced wrist disease. Arthroplasty has enjoyed considerable success in other joints in the body. However, there remains a preference for treating advanced cases of osteoarthritis in the wrist with some type of arthrodesis instead of a total wrist arthroplasty (TWA). This preference exists in spite of the fact that most arthrodeses limit range of motion by almost 50% relative to the non-surgical wrist, and in the most extreme case, a total wrist arthrodesis eliminates all wrist motion (Weiss et al. 2007). Despite more than 40 years of experience with TWA (Carlson et al. 1998), the current generation of wrist implants has still failed replace arthrodesis. Ironically, the TWA is recommended for lower demand patients and patients are specifically restricted from various activities including refraining from regularly lifting more than 10lbs. For those that choose a TWA, there continue to be complications associated with higher rates of failure and revision as compared to arthrodesis (Cavaliere et al. 2008). A major limitation with the current generation of TWA is that they are ellipsoidal designs, based on two independent orthogonal planes of motion: flexion/extension and radial/ulnar deviation. This design is based on a long history of measuring and reporting wrist motion in terms of these two planes. However, alternative planes of wrist motion have been suggested as being more physiologically relevant. By studying the wrist under more functional and loaded conditions, we hope to gain greater insight into the function of the wrist. Such insight could be incorporated into the next generation of wrist implants, such that they might be better able to mimics the function of the normal human carpus. By changing from an artificial wrist designed to rotate about arbitrary axes to one designed to rotate about a physiologic axis, the next generation of TWA could achieve results that surpass arthrodesis.

Carpal Anatomy. The wrist is a uniquely complex joint. Composed of 8 small multi-articular bones, the wrist is situated between the radius and ulna of the forearm and the five metacarpals of the palm. The carpus is an almost entirely passive joint, with only a portion of a single tendon from the carpi ulna extensor inserting on the hook of the hamate and the pisiform. The remaining tendons controlling wrist motion insert on the metacarpals and phalanges.

Markerless Bone Registration (MBR) is an established method for accurately measuring carpal kinematics (Wolfe et al. 1997; Crisco et al. 1998; Crisco et al. 1999; Crisco et al. 2001; Marai et al. 2003; Marai et al. 2006). There are significant challenges in accurately studying the kinematics of the wrist. The small size of the carpus and the complex 3-D motions of each bone make it incredibly difficult to study. External surface markers cannot track the motion of individual carpal bones, only overall wrist motion. Studies of carpal kinematics using more invasive markers are harder to perform and additionally run the risk of affecting the carpal kinematics that we are interested in studying. Based on serial static CT scans, MBR is a non-invasive means of accurately measuring the 3-D kinematics of the entire carpus. The accuracy of this methodology has been established as better than 0.5mm in translation and 1° in rotation using a 0.97mm x 0.97mm x 1mm volume set. This accuracy is improved by almost 50% when using a 0.3mm x 0.3mm x 1mm volume (Neu et al. 2000; Marai et al. 2006). In addition to carpal kinematics, this method has been shown effective at measuring the kinematics of the distal radioulnar joint (DRUJ) (Moore et al. 2002). The details of this methodology are explained in greater detail in section D2c.

The Dart Throwing Motion (DTM) has been described as the most important functional plane of wrist motion. (Moritomo et al. 2007) Traditionally, kinematic studies of the wrist have been focused on the orthogonal flexion/extension and radial/ulnar deviation motions. During wrist flexion/extension, the scaphoid and lunate are known to flex and extend with the wrist. During wrist radial/ulnar deviation, both bones continue to rotate in the flexion/extension plane; flexing during wrist radial deviation and extend during wrist ulnar deviation (Fick 1911; Short et al. 1997; Patterson et al. 1998; Wolfe et al. 2000; Moojen et al. 2002). In 1985, Palmer *et al* measured wrist motion during tasks of daily living and was able to show that a great many tasks involve a motion from radial extension to ulnar flexion, which they described as the *Dart Thrower's Motion* (DTM) (Palmer et al. 1985). Since then, it has been shown that the scaphoid and lunate rotate less during the DTM than during pure flexion/extension or radial/ulnar deviation (Ishikawa et al. 1999; Werner et al. 2004; Crisco et al. 2005). The DTM has been hypothesized to have played a role in human evolution (Wolfe et al. 2006). Used in activities such as throwing rocks, wielding a club, throwing a spear and hammering, the DTM has been shown to be the direction in which the wrist has its greatest overall range of motion (Li et al. 2005). Despite the importance of the DTM, there are still a limited number of studies that have targeted this motion.

Measuring *In Vivo* carpal kinematics during simulated hammering (Specific Aim 1)

Hammering is a forceful occupational task accomplished via extension of the shoulder and elbow and use of the DTM at the wrist. Wrist motion during hammering has been measured using external markers in two different studies. Palmer *et al* was able to show that hammering uses the DTM and that hammering occurs almost entirely in extension (Palmer et al. 1985). Schoenmarklin *et al* measured the effects of handle angle on wrist motion and performance during hammering (Schoenmarklin et al. 1989). Wrist motion was tracked using an external "wrist monitor" that was attached to the distal forearm and tracked the motion of the 2^{nd} and 4^{th} proximal phalanges. While they found that both hammer handle angle and the type of hammering affected the range of motion as well as the ratio of flexion/extension to radial/ulnar deviation all hammering took place in extension and followed the DTM. However, both of these studies used external tracking device which prevent them from measuring the motion of individual carpal bones.

While the kinematics of the carpus during the DTM has been measured *in vitro* (Ishikawa et al. 1999; Werner et al. 2004), only a single study has specifically targeted the DTM *in vivo*. Moritomo *et al* measured carpal motion *in vivo* during a DTM using an MRI based markerless bone-registration technique (Moritomo et al. 2006). The subjects in this study had their wrists imaged at 6 targeted positions from 60° of radial extension to 40° of ulnar flexion. These wrist positions follow the DTM from radial extension to ulnar extension and the rotation of the scaphoid and lunate were both reduced. However, this path of wrist motion is most likely *not* the path associated with hammering.

Prior *in vivo* hammering studies (Palmer et al. 1985; Schoenmarklin et al. 1989) have established that hammering takes place almost entirely in extension, while Moritomo *et al* appear to have targeted a path of wrist motion almost evenly divided between extension and flexion. Based on this information, it appears that they measured kinematics in a path parallel to hammering, but still distinct from the true hammering path. Our study would prove unique, in that it would be the first time kinematics of the carpus were measured during an actual function task.

Static hammering can be used to simulate dynamic hammering. Curran *et al* found that wrist motion during static hammering and dynamic hammering followed similar paths (Curan et al. 2007). They measured the kinematics of wrist relative to the forearm using MTx Inertial Measurement Units (IMU) (Xsens Technologies B.V., The Netherlands) in 11 healthy male volunteers. Based on these results, we feel confident that results obtained during a simulated hammering study are applicable to dynamic hammering.

***In Vivo* measurements of carpal motion during functional tasks are critical to our understanding of carpal function.** This understanding of carpal function has relevance for both basic scientists and clinicians alike. Improved knowledge of carpal kinematics during functional tasks that utilize the DTM could impact what treatments are used for certain patients. Because rotation at the radiocarpal joint is minimized during the DTM, it has been suggested that a radio-scapho-lunate fusion could be more appropriate for patients with arthritis at the radiocarpal joint. (Moritomo et al. 2007) Rehabilitation protocols can also be affected by our understanding of carpal kinematics. By allowing limited motion along the DTM, it might possible to introduce early rehabilitation to the wrist while minimizing motion at an injured radiocarpal joint.

Carpal changes under load. (Specific Aim 2)

A complete understanding the wrist is dependent upon understanding not only how the unloaded wrist moves, but also how it handles load. Under normal conditions the healthy wrist must be able to deal with both compressive and tensive loads. To date, most research on the carpus under load has been focused on radiocarpal joint contact area and pressure distribution using a variety of invasive techniques. Earlier work was performed primarily *in vitro* using FujiFilm to measure the contact center and the contact area of the radioscaphoid and the radiolunate joints. These authors found that joint contact was limited to only 20% of the overall joint surface in both joints. The ratio of scaphoid contact area to lunate contact area was on average 1.47. (Viegas et al. 1987; Kazuki et al. 1991) Two groups developed their own custom sensors to measure joint contact pressure and areas, using sensors that were 1mm and 1.6mm thick respectively. (Hara et al. 1992; Rikli et al. 2007) Hara *et al* established that 15% of load was carried by the ulna and 85% by the radius, of which almost 2/3 was from the scaphoid and 1/3 from the lunate. Rikli *et al* only measured a single *in vivo* wrist and found an almost even distribution of load between the radius and the ulna. It is unknown what effect inserting a 1mm or 1.6mm thick sensor has on the forces being recorded. The effect of compressive loading on carpal motion has only been examined in a single study. Kobayashi *et al* applied an axial load of 98N to 13 cadaver wrists with the wrist fixed in the neutral position. They found that compressive loading caused the scaphoid and lunate to rotate on average 5.1° and 4.2° respectively. These results are hard to extrapolate to the *in vivo* carpus because of the artificial constraint on wrist motion as well as the non-physiologic distribution of force among the tendons of the wrist. Our study will enable us to measure these changes *in vivo* and eliminate many of these confounding factors.

Computer models have been used to estimate force transmission through the wrists in both 2-D and 3-D using various methods. (Schuind et al. 1995; Iwasaki et al. 1998; Carrigan et al. 2003). While these computational models are impressive, they are almost entirely based on a single bone model of the unloaded wrist. Without a second position to measure changes from the first position, it is incredibly difficult to develop and test such models. Only two studies have used multiple positions of the same wrist in their models. The first study estimated *in vivo* cartilage contact area and pressures at the radiocarpal joint before and after gripping a cylinder (Pillai et al. 2007). There are a number of shortcomings to their study; including the use of an untested kinematic tracking method and making various gross assumptions, such as assuming all cartilage to be uniformly 1mm thick. The second study used wrists in a single unloaded neutral position and a second loaded extension position (Majima et al. 2008). However, with such a large change in wrist posture (almost 90°), it is difficult to differentiate between the effect of loading and the effect of extending the wrist. The development of accurate computer models would be aided by *in vivo* data of the same wrist before and after load. Such information could be used to train and/or to validate such models.

Tensive loads have only been measured in a single cadaveric study (Ishikawa et al. 1999), where the authors demonstrated that distraction reduces radiocarpal motion during extension and increase radiocarpal motion during flexion. The effect of load on the wrist independent of motion was not recorded, nor have these findings been confirmed *in vivo*.

Our work will be able to measure carpal kinematics during three different loaded tasks. By imaging each subject before and after loading, in the same wrist position, we should be able to minimize or eliminate confounding wrist motion. While we are studying a limited number of subjects and positions, this data has long term relevance in our basic understanding of the wrist, the design of the next generation of wrist prostheses, as well as developing better computational models of the wrist. There is additional immediate clinical relevance to this study because wrist distraction is used during surgery as well as in the treatment of a variety of wrist injuries. Distraction can be beneficial by reducing load on articular cartilage or across a fracture site and is used in the treatment of distal radius fractures (Fernandez et al. 2000) . While studies have shown that distraction is associated with a decline in outcome measures (Kaempffe 1996; Kaempffe et al. 2000), it is difficult to interpret and apply those findings without first understanding how distraction affects the wrist.

C. PRELIMINARY DATA

Appendix A1: Calfee RP, Leventhal EL, Wilkerson J, Moore DC, Akelman E, Crisco JJ. Simulated radioscapholunate fusion alters carpal kinematics while preserving dart-thrower's motion. J. Hand Surg 33(4):503-10, 2008.

Appendix A2: Leventhal EL, Wolfe SW, Moore DC, Akelman E, Weiss AP, Crisco JJ. Interfragmentary motion in patients with scaphoid nonunion. J. Hand Surg 33(7):1108-15, 2008.

Appendix A3: Moore DC, Crisco JJ, Trafton TG, Leventhal EL. A digital database of wrist bone anatomy and carpal kinematics. J Biomech, 10(1):2537-42, 2007.

Our prior work on both *in vivo* and *in vitro* carpal kinematics demonstrates our ability to measure these complex motions. Using a markerless bone registration methodology previously developed by our group (Crisco et al. 1999; Marai et al. 2006), we were able to measure the 3-D kinematics for the distal forearm, the eight carpal bones as well as the five metacarpals. Using a cadaver model, we were able to show how a simulated radioscapholuate fusion resulted in an increase in midcarpal motion. ((Calfee et al. 2008); Appendix A1)

In a subsequent study on scaphoid non-unions, we demonstrated our ability to use these techniques *in vivo*, as well as adapt them for use in this pathologic state. By studying six subjects with clinically confirmed unilateral scaphoid nonunions, we were able to show significant interfragmentary motion. Further, we were able to demonstrate the motion of the distal fragment was similar to that of the uninjured scaphoid, and that the proximal fragment and the lunate in the injured wrist had significantly less motion than in the uninjured wrist. For this study, the MBR technique was modified to treat each fragment of the injured scaphoid as an individual bone and to track each fragments kinematics independently. The kinematics of the lunate, proximal scaphoid fragment and distal scaphoid fragment in the injured wrist were compared to the kinematics of the intact scaphoid and lunate in the contralateral uninjured wrist. ((Leventhal et al. 2008); Appendix A2)

Absolute forearm position in pronation/supination can be determined from the orientation of the distal radius and ulna alone. Clinically, neutral forearm pronation/supination is defined as the position where the extended thumb is parallel to the humerus with the elbow bent at 90° flexion. At the DRUJ, it is not possible to directly measure the angle of the humerus relative to the wrist. Between the radius and the ulna, only the ulna is rigidly attached to the humerus and can be used as a reference for neutral forearm pronation/supination. By using a slightly modified ulnar coordinate system ((Coburn et al. 2007), see D2c), it was possible to identify the orientation of the ulna using the ulnar styloid. To determine the average offset of the ulnar styloid relative to the humerus, this offset was calculated in seven cadaver arms. Briefly, each cadaver arm included an intact wrist and intact elbow, as well as at least part of the humerus. Each arm was CT scanned with the elbow bent at 90° of flexion. The distal humerus and distal ulna were both segmented manually using Mimics 9.11 (Materialize, Leuven, Belgium). The angular offset between the long axis of the humerus was compared to the y-axis of the ulnar coordinate system. The average offset angle was found to be 172±10°. Based on our observations, the 10° standard deviation represents the variability in human morphology more than an error in our measurements. Using this methodology, we can determine changes in forearm pronation/supination with better than 1° rotational accuracy and the absolute forearm position to within ~10°.

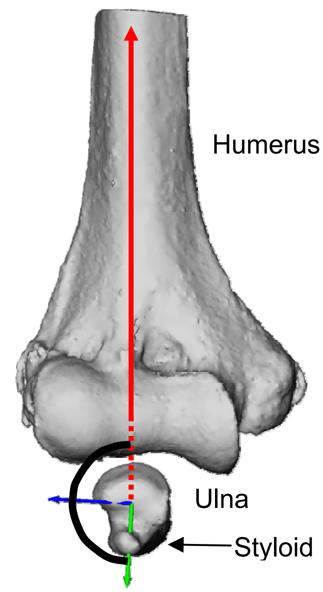

Figure C1-1. The ulnar styloid is oriented 172±10° from the long axis of the humerous (red).

We have experience manipulating and disseminating large volumes of data. This group's past work studying carpal kinematics has resulted in the largest database of *in vivo* carpal kinematics. To share this information and provide increased opportunities for the global study of the carpus, a significant portion of this database was made available online. ((Moore et al. 2007); Appendix A3) Extensive efforts were made to verify the data being disseminated, and to clearly document the file formats used. The end result was the kinematic data for 30 healthy subjects, comprised of over 2,000 files and 2GB of data, available for download. Upon completion of this study, our goal is to produce a similar database in a compatible format that would similarly be available for download. Such a public database could prove extremely beneficial for groups looking to create more accurate computer models of the wrist (Schuind et al. 1995; Carrigan et al. 2003; Pillai et al. 2007; Majima et al. 2008), as well as those trying to understand the properties of wrist ligaments and cartilage (Marai et al. 2006; Crisco et al. 2007; Rainbow et al. 2007; Moritomo et al. 2008; Rainbow et al. 2008).

D. RESEARCH DESIGN AND METHODS

Project Overview

The objective of this study is to gain a better understanding of the *in vivo* 3-D kinematics of the carpus during functional tasks under various types of load. This objective will be realized by studying the kinematics of the forearm, carpus and metacarpals in 14 healthy subjects during 4 specific tasks. The first task, a simulated hammering task, is designed to represent an important functional wrist motion hypothesized to utilize a unique carpal pattern of motion (Aim1). The remaining tasks are divided between common activity of pushing and pulling. Two tensive tasks, or pulling tasks, will be performed both without load and under load to understand how the carpus and the muscles of the forearm work to help carry loads. A single compressive task, or pushing task, will be performed to understand the effect of loading on the interbone spacing in the wrist (Aim 2).

D1. Research Design

D1a. Specific Aim 1. *To determine the kinematics of the wrist and forearm during simulated hammering.*

Objective and Rationale, The objective of the first Aim is to measure the path of wrist motion and rotation at the radiocarpal joint during a simulated hammering task. Hammering is a dominant task involving extension of the shoulder and elbow and the DTM at the wrist (Schoenmarklin et al. 1989). Previous studies have shown that rotation of the scaphoid and lunate are minimized during the DTM (Werner et al. 2004; Crisco et al. 2005; Moritomo et al. 2006), however this has never been confirmed *in vivo* during a functional task. Understanding the kinematics of the carpus during functional tasks can be applied towards design of ergonomic tools as well as designing rehabilitation protocols designed to isolate the midcarpal joint while minimizing motion at the radiocarpal joint.

Experimental Design. 14 healthy, right-hand dominant volunteers (age 18-45) will be CT scanned performing a simulated hammering motion. Using a custom jig, the volunteers will target 5 positions throughout the hammering swing. Carpal kinematics of the distal forearm, carpus and metacarpals will be calculated used an established markerless bone registration (MBR) methodology. Wrist position will be calculated by the orientation of the 3rd metacarpal relative to a radius based coordinate system. Rotation of the scaphoid and lunate will be calculated using Helical Axes of Motion (HAM).

Hypothesis Testing and Anticipated Results. **Hypothesis 1.1:** *Wrist motion follows the DTM during a simulated hammering task.* We will use a hierarchical linear model (HLM) to calculate the ratio of flexion/extension to radial/ulnar deviation for each individual as well as across all subjects. The HLM will report the overall ratio and variability as well as test for the significance of the coupling ratio. We expect all subjects hammering motion to be linear and to follow the previously defined DTM (Crisco et al. 2005).
Hypothesis 1.2: *During the hamming task, there is zero rotation of the scaphoid or lunate.* For each bone, a HLM will be constructed to test total bone rotation as a function of flexion/extension and radial/ulnar deviation from the neutral hammering position. Based on this labs prior analysis of the DTM (Crisco et al. 2005), we believe that there is a path for each individual in which there is no scaphoid and no lunate rotation.

Potential Problems and Alternate Approaches. Due to our experience, we expect no difficulties in the image processing and calculation of the 3-D kinematics of the wrist.

Despite our careful planning, it is possible that the ratio of flexion/extension to radial/ulnar deviation will vary across subjects. (Hypothesis 1.1) Similarly, it is possible that despite wrist motion following the DTM, there will remain significant rotation of the scaphoid and/or lunate. (Hypothesis 1.2) If this is the case, we will examine the relationship between the hammering path and the amount of residual scaphoid and lunate rotation. This relationship will be established using a "bent-stick" linear regression under the assumption that there is a path of minimal scaphoid and lunate rotation, and that deviation from that path will lead to increased rotation.

Due to our sample size of 14 subjects, and the number of variables being tested, it might be difficult to establish the relationship between flexion/extension and radial/ulnar deviation and scaphoid or lunate rotation in a single HLM. (Hypothesis 1.2) If we lack power, we can perform the analysis using flexion/extension as the only independent variable and remove radial/ulnar deviation from the model. Prior studies of the DTM have shown that flexion/extension is the dominant motion (see b2.1 (Werner et al. 2004; Crisco et al. 2005)), so it is the next logic choice to use as the independent variable for the HLM.

D1b. Specific Aim 2. *Measure the change in carpal kinematics during compressive and tensive tasks. Each task is to be performed both with and without load.*

<u>Objective and Rationale,</u> The objective of our second Aim is to observe the effect of compressive and tensive loads on the carpus. The wrist is subject to similar types of loads in various pushing and pulling activities. Most studies to date on compressive and tensive loads in the carpus have been performed using cadavers and pressure sensing film or implants at the radiocarpal joint. To date, no one has measured these loads affects the spacing of the carpus *in vivo* using a noninvasive technique. By using an *in vivo* model, we have eliminated the enormous complexity associated with trying to replicate the appropriate muscle tone and loading that is used to balance the wrist. Knowledge of how the wrist deals with these loads is important if we wish to completely understand the function of the wrist. Such knowledge can be applied towards designing computer models of the wrist, understanding the mechanical properties of the carpal ligaments. Understanding the wrist under tension has more direct clinical applicability, by helping to determine why patients respond differently to traction which is used for a variety of procedures.

<u>Experimental Design.</u> The same 14 volunteers from Aim 1 will be used for Aim 2. Each volunteer will perform two tensive tasks and single compressive task each without load and under a static load (98N). One tensive task will be accomplished with the volunteer grasping a radiotranslucent grip and using their forearm muscles, while the second tensive task will use nylon finger traps to allow the volunteer to relax their forearm muscles. The compressive task will also be performed without load and under the same static load of 98N. Carpal kinematics of the distal forearm, carpus and metacarpals will be calculated using the same (MBR) methodology as Aim 1.

Interbone spacing will be calculated at three joints: the radiocarpal joint will be represented by the radius and the lunate, the midcarpal joint will be represented by the lunate and the capitate, and the carpal-metacarpal joint will be represented by the capitate and the 3rd metacarpal. Distances between the joints specified will be calculated in the x-axis of the radial based coordinate system, or in the orientation of the long axis of the forearm.

<u>Hypothesis Testing and Anticipated Results.</u> **Hypothesis 2.1:** *Tensive loading of the wrist without gripping causes equal separation at the radiocarpal, midcarpal, and carpal-metacarpal joints.*
Hypothesis 2.2: *Tensive loading of the wrist with active gripping causes no separation at the radiocarpal, midcarpal, or carpal-metacarpal joints.*
Hypothesis 2.3: *The distance between the radius and the proximal row is not altered with compressive loading of the extended wrist.*
Changes in interbone spacing for each task will be tested using a two-way repeated measures ANOVA. During the tensive task without gripping, we expect there to be significant changes in interbone spacing at all three joints between the unloaded and loaded trials. We do not expect there to be a significant difference in the magnitude of change between the three joints. Without the assistance of muscle activation, most of the load will be carried by the ligaments of the carpus and the surrounding soft tissue. Clinically it has been shown that 178N of tensile force can cause 16mm of

distraction between the radius and the metacarpals (Volz 1976), so a load of 98N should be more than enough to cause a detectable change. During the tensive task while gripping, we expect there to be no change in interbone spacing at any of the joints. Almost all of the tendons of the forearm muscles completely bridge across the carpus and should carry most the load while gripping. During the compressive task, we do not expect a change in interbone spacing. The largely incompressible cartilage and strong carpal bones should carry the weight without a detectable change in distances.

Potential Problems and Alternate Approaches.

The MBR methodology is well established and we expect no difficulties in calculating the 3-D kinematics of the carpus. However, if there is significant changes in wrist position between the unloaded and loaded scans this will represent a confounding factor in the data. It will be difficult to determine if any change is related to load or the change in wrist position. To prevent this, the time between the unloaded and loaded scans will be kept as short as possible. In pilot scans, we have been able to keep this time to between 30-60 seconds. Additionally, prior to each unloaded trial, the volunteers' wrists will be briefly loaded to allow the wrist to assume its natural position under load. We hope that this will minimize variability between the unloaded and loaded trials. To evaluate the effect of this problem, we will measure the change in wrist position for each subject using the orientation of the 3rd metacarpal relative to the radius.

D2. Methods

D2a. Subject Recruitment.

14 volunteers (7 male, 7 female) will be recruited from both Brown University and Lifespan employees. Recruitment will be performed using both IRB approved flyers as well as IRB approved bulk emails to the Brown Medical School. IRB approval for this study was last approved on October 8, 2008, with an expiration date of October 7, 2009.

Subjects must be between 18 and 45 years old at the time of the study and be free from wrist pain or history of wrist injury. To simplify analysis, all volunteers must be right-hand dominant. After enrollment, each volunteer will receive a history and physical of both wrists by Dr. Akelman, one of the hand surgeons in the department. Subjects will be excluded from the study for any history for any history of wrist fracture, hand surgery. Volunteers cannot have had a soft tissue or ligamentous injury and will be excluded for metabolic diseases that could impact normal wrist function such as severe osteoporosis, hyperthyroidism, etc. Physical exam will include bilateral range of motion measurements using a goniometer, as well as clinical examination for signs of scaphoid instability. Wrist strength will be measured using a hand-held Jamar dynamometer (Smith and Nephew, Memphis, TN) and averaged over three trials for each hand. Bilateral PA, lateral, and AP grip radiographs of the wrist will be used to measure radial inclination, ulnar variance, radial shortening, radial tilt, scapholunate interval, scapholunate angle, radiolunate angle, and capitolunate angles. Subjects will be excluded from the study for abnormal measurements that would indicate the existence of wrist pathology.

D2b. Data Acquisition.

Wrist Tasks and Positioning

Simulated Hammering (Aim 1)

Each volunteer will be scanned in a custom designed jig allowing them to target 5 positions of simulated hammering. This jig will be designed to allow the volunteer to move their wrist through the hammering motion without restriction, while also minimizing motion artifact by providing a rest for the forearm as well as stops for the hammer handle at each position. The neutral hammering position will be defined as the position with the hammer handle perpendicular to the forearm. Windup will be 40° back from neutral and impact is 40° forward from the neutral position. The image collection sequence will follow the natural hammering sequence: 1) -40° (windup), -20°, 0° (neutral), 20°, 40° (impact). Wrist position for this task will be calculated by the orientation of the 3rd metacarpal relative to the radius, as prior work has shown that targeting positions using goniometers, protractors, or external markers to be inaccurate (Wolfe et al. 2000).

Tensive loading while gripping (Aim 2)

Each volunteer will be loaded with a static tensive load of 98N (or 10kg) applied by a deadweight. The 98N load represents what we found to be the maximum load that could be comfortably held by all members of our lab and is a load used in previous studies (Trumble et al. 1987; Kazuki et al. 1991; Hara et al. 1992; Kobayashi et al. 1997).

The volunteer will be positioned prone on the scanning table with their arm extended above their head. The volunteer's shoulder, elbow, and wrist will all be aligned down the center of the scanning table and the direction of the load. We have found this position to be the most comfortable for the subject, minimizing the risk of them moving during scanning and causing motion artifact. Further, this position, allows us to easily standardize on the direction of load being applied to each subject. For both the unloaded and loaded trial, the volunteer will be gripping a radiotranslucent handle. Prior to the unloaded trial, the handle is briefly loaded to allow the wrist to assume its natural position under load and minimize variations in wrist posture between the loaded and unloaded state.

Tensive loading without gripping (Aim 2)

The tensive loading task without gripping will be similar to the previous task (tensive loading while gripping). The primary difference is that instead of applying the load via a handle gripped by the volunteer, the load is applied via a set of nylon finger traps (Instrument Specialists Inc., Boerne, Texas). Nylon finger traps are radiotranslucent and allow the load to be applied to the wrist without requiring the volunteer to grip anything and contract the muscles of their forearm. Imaging will take place both without load (0N) and with the static tensive load applied (98N).

Compressive loading (Aim 2)

For compressive loading, a standard bathroom scale will be mounted vertically in custom jig. Volunteers will be positioned with their palm centered on the scale and their forearm perpendicular to the surface of the scale. Unlike the tensive tasks, where the load was applied by deadweight, the loaded trial of the compressive task will require that they volunteer apply force against the scale and to hold that position. By using a standard bathroom scale, the volunteer has immediate feedback as to how much force they are applying during the loaded trial. Informal experimentation with this setup in our lab has shown that with proper instruction, it is not difficult to apply the 98N force and remain motionless for the short duration of a scan. Care will be taken to ensure that their hand, elbow and shoulder are aligned down the center of the scanning table. Images we be acquired in both the unloaded (0N) state and the loaded state (98N).

CT Imaging (Aims 1 & 2)

CT scanning will be performed in a GE HighSpeed Advantage CT scanner at 80kVp and 80mA. Images for Aim 1 will have a FOV of 25cm and in-plane resolution of 0.6mm x 0.6mm, while images for Aim 2 will have a narrower FOV of 14cm with in-plane resolution of 0.3mm x 0.3mm. All images will be collected at 0.6mm slice intervals and 0.6mm thickness using the BONE PLUS algorithm.

D2c. Measuring 3-D Carpal Kinematics *In Vivo*

3-D kinematics of the radius, ulna, eight carpal bones, and the metacarpals will be measured using a Markerless Bone Registration (MBR) methodology. Using a method developed and advanced by our group (Crisco et al. 1999; Marai et al. 2006), our MBR methodology provides a semi-automated method for *in vivo* measurements of carpal kinematics. Briefly, the cortical shell of each bone is manually segmented using Mimics 9.11 (Materialize, Leuven, Belgium) to produce 3-D bone models. Custom C++ code (GNU gcc, Free Software Foundation, Boston, Massachusetts) is used to track the segmented bones in the subsequent scans. Additional custom Matlab code (Matlab 2007b, The MathWorks, Natick, Massachusetts) is used to register the radii together and eliminate small motions of the forearm between scans. With our planned image resolution of at least 0.6mm x 0.6mm x 0.6mm volume set, our kinematic accuracy should be better than 0.5mm of translational error and 1° rotational error.

Carpal bone rotations are described in a radial based coordinate system. The methodology for establishing a Radial Coordinate System (RCS) is well established (Coburn et al. 2007). The x-axis is defined as a vector running down the long axis of the diaphysis of the radius. The y-axis is a vector perpendicular to the x-axis oriented towards the radial styloid. The z-axis is then the cross product of the x-axis and the y-axis. The origin of the coordinate system is the point where the x-axis intersects the cortical shell of the radius at the radiocarpal joint.

An ulnar coordinate system is defined to allow forearm pronation/supination to be calculated. The ulnar coordinate system is created in a similar manner to the RCS, but has been modified slightly to improve precision and repeatability when used with the smaller distal ulna. The ulna coordinate system is defined with the x-axis oriented down the long axis of the ulnar diaphysis. The z-axis is calculated as the cross product of the x-axis and a vector from the center of the ulnar metaphysis (excluding the styloid) to the center of the ulnar styloid. The y-axis is then calculated as the cross product of the x-axis and the z-axis. The origin of the coordinate system is the point on the surface of the cortical shell where the cortical surface is intersected by a vector parallel to the x-axis, and passing through the centroid of the ulnar metaphysis (excluding the styloid).

Principal inertial axes and centroid locations are calculated for the eight carpal bones and the five metacarpals are calculated from their 3-D objects. Computations are performed using custom Matlab code based on Gauss's divergence theorem assuming a uniform bone density of unit value 1 (Messner et al. 1980; Eberly et al. 1991; Gonzalez-Ochoa et al. 1998). These inertial axes are then oriented according to the method proposed by Coburn *et al* (Coburn et al. 2007).

D2d. Data Analysis and Outcome Measures

<u>Wrist Position</u>

Wrist position will be calculated by the orientation of the 3rd metacarpal's long inertial axis relative to the RCS ((Coburn et al. 2007), see D2c), as prior work has shown that targeting positions using goniometers, protractors, or external markers to be inaccurate (Wolfe et al. 2000).

<u>Carpal Bone Rotation</u>

Bone rotations are represented using Helical Motions of Axes (HAM) variables. (Panjabi et al. 1981). HAM variables can be used to describe any rigid body transformation between two discrete positions. Transformations are described as a rotation about and a translation along a unique axis in space. Magnitudes of rotation are kept positive by adjusting the direction of unique axis such that is oriented correctly according to the right hand rule.

<u>Relative Bone Translation</u>

Relative bone translation will be calculated at three joints: the radiocarpal joint, the midcarpal joint and the carpal-metacarpal joint (Aim 2). Relative bone position at the radiocarpal joint will be defined as the distance between the origin of the RCS (see D2c) and the centroid of the lunate. The midcarpal joint will be defined as the distance between the centroid of the lunate and the centroid of the capitate. Finally, the carpal-metacarpal joint will be defined as the distance between the centroid of the capitate and a point manually selected on the proximal end of the 3rd metacarpal. The point on the 3rd metacarpal will be located on the surface of the cortical shell, and the center of the capitate articulating surface using Wrist Visualizer (custom application written in C# and C++ (Visual Studio .NET 2005, Microsoft, Redmond WA) using the Coin3D graphics library (Kongsberg SIM, Sandvika, Norway)). Manual point selection will only occur once per subject, so minor variations in point selection should have minimal affect on the final results which are based on the relative change of the same point. Translation of bone positions will be measured along the x-axis of the radial coordinate system, or in the direction of the long axis of the forearm.

Joint Space Centroid

The joint space centroid approximates the center of contact between two bones. Contours of interbone distances will be created using a combination of custom C++ code and Wrist Visualizer. Contours will be computed on the cortical surface of a reference bone, defining the area on that surface which is located within a specified distance threshold from a second test bone. The joint space centroid is the centroid of that contour, which is calculated and placed on the surface of the reference bone. These contours will be calculated for multiple wrist positions and can show changes in the location of that centroid. Because we will be using bone models without cartilage surfaces, this centroid does not represent the true center of contact between the bones; however, the change in location of that centroid should be representative of how the center of contact is moving. Selection of the distance threshold will be determined from experimental data. A range of reasonable distances that estimate the combined thickness of the cartilage surfaces will be evaluated in the neutral wrist position. Given our knowledge of joint anatomy, we expect there to be a subset of ranges for which there is virtually no change in locate of the contour centroid. The midpoint of that range will be used as the distance threshold.

D2e. Statistical Analysis

Specific Aim 1. *To determine the kinematics of the wrist and forearm during simulated hammering.*
Hypothesis 1.1: *Wrist motion follows the DTM during a simulated hammering task.*
A single hierarchical linear model (HLM) (Bryke et al. 1992) will be used to test if there is a relationship between flexion/extension and radial/ulnar deviation during hammering. The HLM will provide estimates of the between-subject variability as well as the significance of the coupling ratio.
Power Analysis: Due to cost and time considerations we are limited to 14 subjects for the study. Power analysis was designed to compare the slope of the regression or the coupling ratio to the t distribution, as is the case for the fixed-effect estimate of slope in HLM. Power was estimated for a 2-tailed alpha of 0.05. Given this sample size, we will be able to detect an effect size (Cohen's *d*) of 1.2 with a power of 0.80. Assuming a standard deviation of 0.15 (~4°) in the slopes, we will be able to detect a slope of approximately 0.18.

Hypothesis 1.2: *During the hamming task, there is zero rotation of the scaphoid or lunate.*
Significant rotation of each bone will be tested using an HLM for each bone. Each HLM will test if there is a relationship between wrist flexion/extension & radial/ulnar deviation motions and overall

bone rotation. As with Hypothesis 1.1, the HLM will provide estimates of the between-subject variability as well as the significance of the relationship between wrist motion and bone rotation.

Power Analysis: Given our 14 subject limitation and a similar HML model as Hypothesis 1.1, we will be able to detect an effect size (Cohen's *d*) of 1.2 with a power of 0.80. This should allow us to detect bone rotation as small as 6% of overall wrist motion given a standard deviation of 5%.

Specific Aim 2. *Measure the change in carpal kinematics during compressive and tensive tasks. Each task is to be performed both with and without load.*

Hypothesis 2.1: *Tensive loading of the wrist without gripping causes equal separation at the radiocarpal, midcarpal, and carpal-metacarpal joints.*

Hypothesis 2.2: *Tensive loading of the wrist with active gripping causes no separation at the radiocarpal, midcarpal, or carpal-metacarpal joints*

Hypothesis 2.3: *The distance between the radius and the proximal row is not altered with compressive loading of the extended wrist.*

For each task, changes in relative bone translation for each tensive task will be tested using a two-way repeated measures ANOVA. 12 comparisons will be incorporated into the analysis:

Test for significant relative bone translation due to loading X 3 joints	3
Test for difference in the unloaded relative bone positions between the 3 joints	3
Test for difference in the loaded relative bone positions between the 3 joints	3
Test for difference in the change in relative bone translation between the 3 joints	3
Total	12

While we do not expect meaningful differences for the 2nd and 4th sets of statistical tests, they were included for completeness.

Power Analysis: Using the same 14 subjects from Aim 1, power analysis was performed to calculate the minimum magnitude of translational we should be able to detect. Hypothesis testing will be performed using orthogonal constructs and tested against the t distribution. To maintain an overall alpha of 0.05 across all hypotheses, alpha was adjusted for the 12 hypotheses using the Bonferroni correction. Estimating the within subject correlation to be r=0.5, we should be able to detect an effect size (Cohen's *d*) of 1.1 with a power of 0.80. This translates to detecting a translation of 0.30mm differences in distances given a standard deviation of 0.28mm.

E. LITERATURE CITED

Bryke, A. S. and Raudenbush, S. W. (1992). *Hierarchical Linear Models: Applications and Data Analysis Methods*. Thousand Oaks, CA, Sage Publications.

Calfee, R. P., Leventhal, E. L., Wilkerson, J., Moore, D. C., Akelman, E. and Crisco, J. J. (2008). "Simulated radioscapholunate fusion alters carpal kinematics while preserving dart-thrower's motion." *J Hand Surg [Am]* **33**(4): 503-10.

Carlson, J. R. and Simmons, B. P. (1998). "Total wrist arthroplasty." *J Am Acad Orthop Surg* **6**(5): 308-15.

Carrigan, S. D., Whiteside, R. A., Pichora, D. R. and Small, C. F. (2003). "Development of a three-dimensional finite element model for carpal load transmission in a static neutral posture." *Ann Biomed Eng* **31**(6): 718-25.

Cavaliere, C. M. and Chung, K. C. (2008). "A systematic review of total wrist arthroplasty compared with total wrist arthrodesis for rheumatoid arthritis." *Plast Reconstr Surg* **122**(3): 813-25.

Coburn, J. C., Upal, M. A. and Crisco, J. J. (2007). "Coordinate systems for the carpal bones of the wrist." *J Biomech* **40**(1): 203-9.

Crisco, J. J., Coburn, J. C., Moore, D. C., Akelman, E., Weiss, A. P. and Wolfe, S. W. (2005). "In vivo radiocarpal kinematics and the dart thrower's motion." *J Bone Joint Surg Am* **87**(12): 2729-40.

Crisco, J. J. and McGovern, R. D. (1998). "Efficient calculation of mass moments of inertia for segmented homogeneous three-dimensional objects." *J Biomech* **31**(1): 97-101.

Crisco, J. J., McGovern, R. D. and Wolfe, S. W. (1999). "Noninvasive technique for measuring in vivo three-dimensional carpal bone kinematics." *J Orthop Res* **17**(1): 96-100.

Crisco, J. J., Pike, S., Hulsizer-Galvin, D. L., Akelman, E., Weiss, A. P. and Wolfe, S. W. (2003). "Carpal bone postures and motions are abnormal in both wrists of patients with unilateral scapholunate interosseous ligament tears." *J Hand Surg [Am]* **28**(6): 926-37.

Crisco, J. J., Rainbow, M. J., Moore, D. C., Akelman, E. and Wolfe, S. W. (2007). *Elongation of the Radioscaphocapitate (RSC) Ligament During Wrist Flexion/Extension and Ulnar/Radial Deviation*. Annual Meeting of the Orthopaedic Research Society, San Diego, CA.

Crisco, J. J., Wolfe, S. W., Neu, C. P. and Pike, S. (2001). "Advances in the in vivo measurement of normal and abnormal carpal kinematics." *Orthop Clin North Am* **32**(2): 219-31, vii.

Curan, P. F., Rainbow, M. J., Moore, D. C. and Crisco, J. J. (2007). *Hammering and Dart Throwing are Kinematically Different*. American Society of Biomechanics, Stanford University, Stanford, CA.

Eberly, D., Lancaster, J. and Alyassin, A. (1991). "On gray scale image measurements: II. Surface area and volume." *CVGIP: Graphical Models and Image Processing* **53**(6): 550-562.

Fernandez, D. L. and Mader, K. (2000). "The treatment of complex carpal dislocations by external fixation." *Injury* **31 Suppl 1**: 92-101.

Fick (1911). *Handbuch der Anatomie und Mechanik der Gelenke,*, Fischer, Jena.

Gonzalez-Ochoa, C., McCammon, S. and Peters, J. (1998). "Computing Moments of Objects Enclosed by Piecewise Polynomial Surfaces." *ACM Transactions on Graphics (TOG)* **17**(3): 143-157.

Hara, T., Horii, E., An, K. N., Cooney, W. P., Linscheid, R. L. and Chao, E. Y. (1992). "Force distribution across wrist joint: application of pressure-sensitive conductive rubber." *J Hand Surg [Am]* **17**(2): 339-47.

Ishikawa, J., Cooney, W. P., 3rd, Niebur, G., An, K. N., Minami, A. and Kaneda, K. (1999). "The effects of wrist distraction on carpal kinematics." *J Hand Surg [Am]* **24**(1): 113-20.

Iwasaki, N., Genda, E., Minami, A., Kaneda, K. and Chao, E. Y. (1998). "Force transmission through the wrist joint in Kienbock's disease: a two-dimensional theoretical study." *J Hand Surg [Am]* **23**(3): 415-24.

Kaempffe, F. A. (1996). "External fixation for distal radius fractures: adverse effects of excess distraction." *Am J Orthop* **25**(3): 205-9.

Kaempffe, F. A. and Walker, K. M. (2000). "External fixation for distal radius fractures: effect of distraction on outcome." *Clin Orthop Relat Res*(380): 220-5.

Kazuki, K., Kusunoki, M. and Shimazu, A. (1991). "Pressure distribution in the radiocarpal joint measured with a densitometer designed for pressure-sensitive film." *J Hand Surg [Am]* **16**(3): 401-8.

Kobayashi, M., Berger, R. A., Nagy, L., Linscheid, R. L., Uchiyama, S., Ritt, M. and An, K. N. (1997). "Normal kinematics of carpal bones: a three-dimensional analysis of carpal bone motion relative to the radius." *J Biomech* **30**(8): 787-93.

Leventhal, E. L., Wolfe, S. W., Moore, D. C., Akelman, E., Weiss, A. P. and Crisco, J. J. (2008). "Interfragmentary motion in patients with scaphoid nonunion." *J Hand Surg [Am]* **33**(7): 1108-15.

Li, Z. M., Kuxhaus, L., Fisk, J. A. and Christophel, T. H. (2005). "Coupling between wrist flexion-extension and radial-ulnar deviation." *Clin Biomech (Bristol, Avon)* **20**(2): 177-83.

Majima, M., Horii, E., Matsuki, H., Hirata, H. and Genda, E. (2008). "Load transmission through the wrist in the extended position." *J Hand Surg [Am]* **33**(2): 182-8.

Marai, G. E., Crisco, J. J. and Laidlaw, D. H. (2006). "A kinematics-based method for generating cartilage maps and deformations in the multi-articulating wrist joint from CT images." *Conf Proc IEEE Eng Med Biol Soc* **1**: 2079-82.

Marai, G. E., Laidlaw, D. H., Coburn, J. C., Upal, M. A. and Crisco, J. J. (2003). *A 3D Method for Segmenting and Registering Carpal Bones from CT Volume Images*. Annual Meeting of the American Society of Biomechanics, Toledo, OH.

Marai, G. E., Laidlaw, D. H. and Crisco, J. J. (2006). "Super-resolution registration using tissue-classified distance fields." *IEEE Trans Med Imaging* **25**(2): 177-87.

Messner, A. M. and Taylor, G. Q. (1980). "Algorithm 550: Solid Polyhedron Measures [Z]." *ACM Transactions on Mathematical Software (TOMS)* **6**(1): 121-130.

Moojen, T. M., Snel, J. G., Ritt, M. J., Kauer, J. M., Venema, H. W. and Bos, K. E. (2002). "Three-dimensional carpal kinematics in vivo." *Clin Biomech (Bristol, Avon)* **17**(7): 506-14.

Moore, D. C., Crisco, J. J., Trafton, T. G. and Leventhal, E. L. (2007). "A digital database of wrist bone anatomy and carpal kinematics." *J Biomech* **40**(11): 2537-42.

Moore, D. C., Hogan, K. A., Crisco, J. J., 3rd, Akelman, E., Dasilva, M. F. and Weiss, A. P. (2002). "Three-dimensional in vivo kinematics of the distal radioulnar joint in malunited distal radius fractures." *J Hand Surg [Am]* **27**(2): 233-42.

Moritomo, H., Apergis, E. P., Herzberg, G., Werner, F. W., Wolfe, S. W. and Garcia-Elias, M. (2007). "2007 IFSSH committee report of wrist biomechanics committee: biomechanics of the so-called dart-throwing motion of the wrist." *J Hand Surg [Am]* **32**(9): 1447-53.

Moritomo, H., Murase, T., Arimitsu, S., Oka, K., Yoshikawa, H. and Sugamoto, K. (2008). "Change in the length of the ulnocarpal ligaments during radiocarpal motion: possible impact on triangular fibrocartilage complex foveal tears." *J Hand Surg [Am]* **33**(8): 1278-86.

Moritomo, H., Murase, T., Goto, A., Oka, K., Sugamoto, K. and Yoshikawa, H. (2006). "In vivo three-dimensional kinematics of the midcarpal joint of the wrist." *J Bone Joint Surg Am* **88**(3): 611-21.

Neu, C. P., McGovern, R. D. and Crisco, J. J. (2000). "Kinematic accuracy of three surface registration methods in a three-dimensional wrist bone study." *J Biomech Eng* **122**(5): 528-33.

Palmer, A. K., Werner, F. W., Murphy, D. and Glisson, R. (1985). "Functional wrist motion: a biomechanical study." *J Hand Surg [Am]* **10**(1): 39-46.

Panjabi, M. M., Krag, M. H. and Goel, V. K. (1981). "A technique for measurement and description of three-dimensional six degree-of-freedom motion of a body joint with an application to the human spine." *J Biomech* **14**(7): 447-60.

Patterson, R. M., Nicodemus, C. L., Viegas, S. F., Elder, K. W. and Rosenblatt, J. (1998). "High-speed, three-dimensional kinematic analysis of the normal wrist." *J Hand Surg [Am]* **23**(3): 446-53.

Pillai, R. R., Thoomukuntla, B., Ateshian, G. A. and Fischer, K. J. (2007). "MRI-based modeling for evaluation of in vivo contact mechanics in the human wrist during active light grasp." *J Biomech* **40**(12): 2781-7.

Rainbow, M. J., Crisco, J. J., Akelman, E. and Wolfe, S. W. (2008). *Elongation of the Extrinsic Radiocarpal Ligaments of a Subject-Specific Kinematically Driven Articular Model of the Carpus During Wrist Flexion/Extension*. Annual Meeting of the Orthopaedic Research Society, San Francisco, CA.

Rainbow, M. J., Crisco, J. J., Moore, D. C., Akelman, E. and Wolfe, S. W. (2007). *A Method for Modeling Ligament Fibers in the Carpus*. Annual Meeting of the International Society of Ligament and Tendons, San Diego, CA.

Rikli, D. A., Honigmann, P., Babst, R., Cristalli, A., Morlock, M. M. and Mittlmeier, T. (2007). "Intra-articular pressure measurement in the radioulnocarpal joint using a novel sensor: in vitro and in vivo results." *J Hand Surg [Am]* **32**(1): 67-75.
Ryu, J. Y., Cooney, W. P., 3rd, Askew, L. J., An, K. N. and Chao, E. Y. (1991). "Functional ranges of motion of the wrist joint." *J Hand Surg [Am]* **16**(3): 409-19.
Schoenmarklin, R. W. and Marras, W. S. (1989). "Effects of handle angle and work orientation on hammering: I. Wrist motion and hammering performance." *Hum Factors* **31**(4): 397-411.
Schuind, F., Cooney, W. P., Linscheid, R. L., An, K. N. and Chao, E. Y. (1995). "Force and pressure transmission through the normal wrist. A theoretical two-dimensional study in the posteroanterior plane." *J Biomech* **28**(5): 587-601.
Schuind, F., Eslami, S. and Ledoux, P. (2008). "Kienbock's disease." *J Bone Joint Surg Br* **90**(2): 133-9.
Short, W. H., Werner, F. W., Fortino, M. D. and Mann, K. A. (1997). "Analysis of the kinematics of the scaphoid and lunate in the intact wrist joint." *Hand Clin* **13**(1): 93-108.
Short, W. H., Werner, F. W., Green, J. K., Weiner, M. M. and Masaoka, S. (2002). "The effect of sectioning the dorsal radiocarpal ligament and insertion of a pressure sensor into the radiocarpal joint on scaphoid and lunate kinematics." *J Hand Surg [Am]* **27**(1): 68-76.
Trumble, T., Glisson, R. R., Seaber, A. V. and Urbaniak, J. R. (1987). "Forearm force transmission after surgical treatment of distal radioulnar joint disorders." *J Hand Surg [Am]* **12**(2): 196-202.
Viegas, S. F., Tencer, A. F., Cantrell, J., Chang, M., Clegg, P., Hicks, C., O'Meara, C. and Williamson, J. B. (1987). "Load transfer characteristics of the wrist. Part I. The normal joint." *J Hand Surg [Am]* **12**(6): 971-8.
Volz, R. G. (1976). "The development of a total wrist arthroplasty." *Clin Orthop Relat Res*(116): 209-14.
Watson, H. K. and Ballet, F. L. (1984). "The SLAC wrist: scapholunate advanced collapse pattern of degenerative arthritis." *J Hand Surg [Am]* **9**(3): 358-65.
Weiss, K. E. and Rodner, C. M. (2007). "Osteoarthritis of the wrist." *J Hand Surg [Am]* **32**(5): 725-46.
Werner, F. W., Green, J. K., Short, W. H. and Masaoka, S. (2004). "Scaphoid and lunate motion during a wrist dart throw motion." *J Hand Surg [Am]* **29**(3): 418-22.
Wolfe, S. W., Crisco, J. J. and Katz, L. D. (1997). "A non-invasive method for studying in vivo carpal kinematics." *J Hand Surg [Br]* **22**(2): 147-52.
Wolfe, S. W., Crisco, J. J., Orr, C. M. and Marzke, M. W. (2006). "The dart-throwing motion of the wrist: is it unique to humans?" *J Hand Surg [Am]* **31**(9): 1429-37.
Wolfe, S. W., Neu, C. and Crisco, J. J. (2000). "In vivo scaphoid, lunate, and capitate kinematics in flexion and in extension." *J Hand Surg [Am]* **25**(5): 860-9.

F. Current Status

F1. Overview

Aim 1

- Custom Jig Design and Construction: Completed
- Volunteer Recruitment: Completed
- Volunteer Scanning: Completed
- Image Segmentation & Processing: Completed
- Data Analysis: Mostly completed. We are currently working to update the statistical analysis
- Publication of results: Abstract submitted on August 18, 2008, for presentation at the 55th Annual Meeting of the Orthopaedic Research Society (ORS) (See Appendix A4). Manuscript in progress.

Aim 2

- Custom Jig Design and Construction: Completed
- Volunteer Recruitment: Completed
- Volunteer Scanning: Completed
- Image Segmentation & Processing: Completed
- Data Analysis: In progress.
- Publication of results: Preliminary results submitted on August 18, 2008, for presentation at the 55th Annual Meeting of the Orthopaedic Research Society (ORS) (See Appendix A5).

F2. Results

Aim 1

The hammering motion follows the DTP. The average coupling ratio, or ratio of flexion/extension to radial/ulnar deviation during hammering was 1.2. This means that for every 10° of wrist ulnar deviation, there was ~12° of wrist flexion. The standard error of the regression was 0.1. (Figure F2-1) Forearm pronation/supination during hammering was minimal, averaging of only 12° rotation throughout the entire motion. The average coupling ratio between flexion/extension and pronation/supination was -0.15±0.3, meaning that for every 10° of wrist flexion, there was an average of 1.5° of wrist supination. However, while the average motion tended towards supination, there were multiple subjects who pronated during hammering. Additionally, there was a wide range of absolute forearm positions in the neutral hammering position, ranging from almost 40° of pronation to almost 50° of supination.

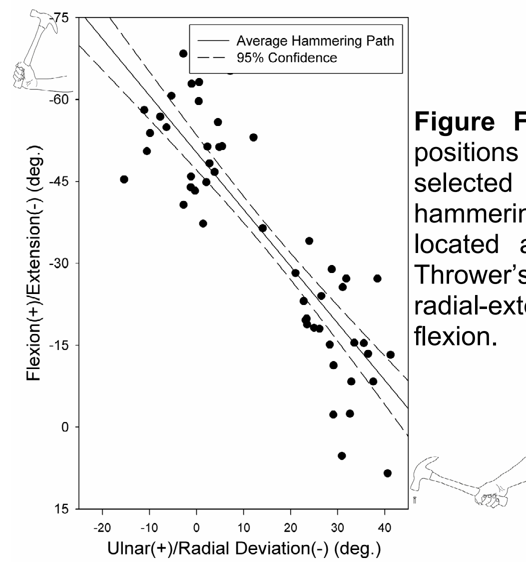

Figure F2-1. The wrist positions the subjects selected during the hammering task were located along the Dart Thrower's Path from radial-extension to ulnar-flexion.

Residual radioscaphoid and radiolunate rotation was 37±10% of overall wrist flexion/extension. Meaning, that for every 10° of wrist flexion, there was 4° of scaphoid rotation. (Figure F2-2)

Deviation from the DTP was associated with an increase in radioscaphoid rotation. Using a bent-stick linear regression, we were able to establish that the DTP with the smallest amount of scaphoid rotation had a coupling ratio of 1.3. At that coupling ratio, the model predicted that the scaphoid will rotate roughly 25% of wrist motion. (Figure F2-3)

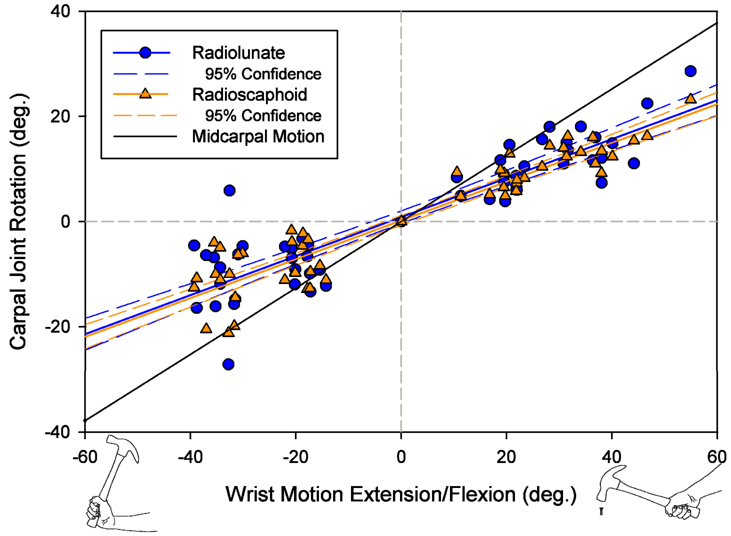

Figure F2-2. Regression revealed that roughly twice as much motion occurred at the midcarpal joint than at the radiocarpal joint during hammering.

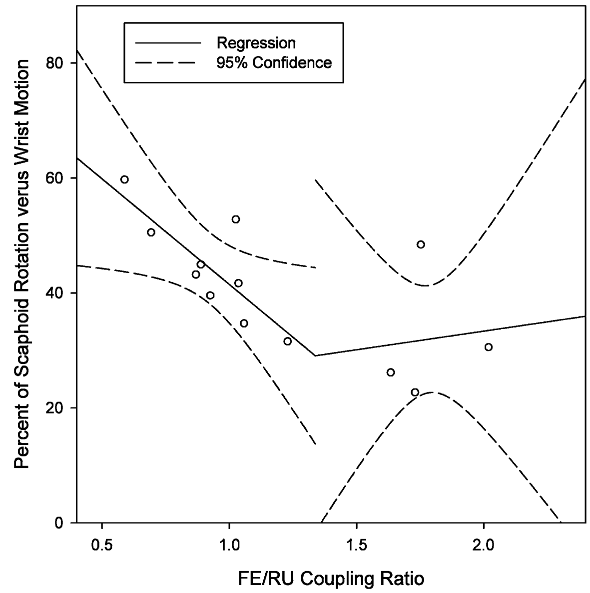

Figure F2-3. Bent stick regression showed that radioscaphoid motion was minimized at a coupling ratio of 1.3 and increased as the hammering path deviated from the DTM.

Aim 2

For the tensive task while gripping, subjects moved their wrists only 7° on average between the unloaded and loaded trial. There was no significant relative bone translation at any of the three joints after loading. (Figure F2-4a)

During the tensive task without gripping, subjects again moved their wrists an average of only 7° between the unloaded and loaded trial. However, there was a significant relative bone translation at the radiocarpal (1.0mm) as well as the midcarpal joints (2.0mm). There was no significant translation at the carpal-metacarpal joint. The amount of translation was significantly different at all three joints. (Figure F2-4b)

Under compression, there was no relative bone translation at the radiocarpal joint. (Figure F2-4c)

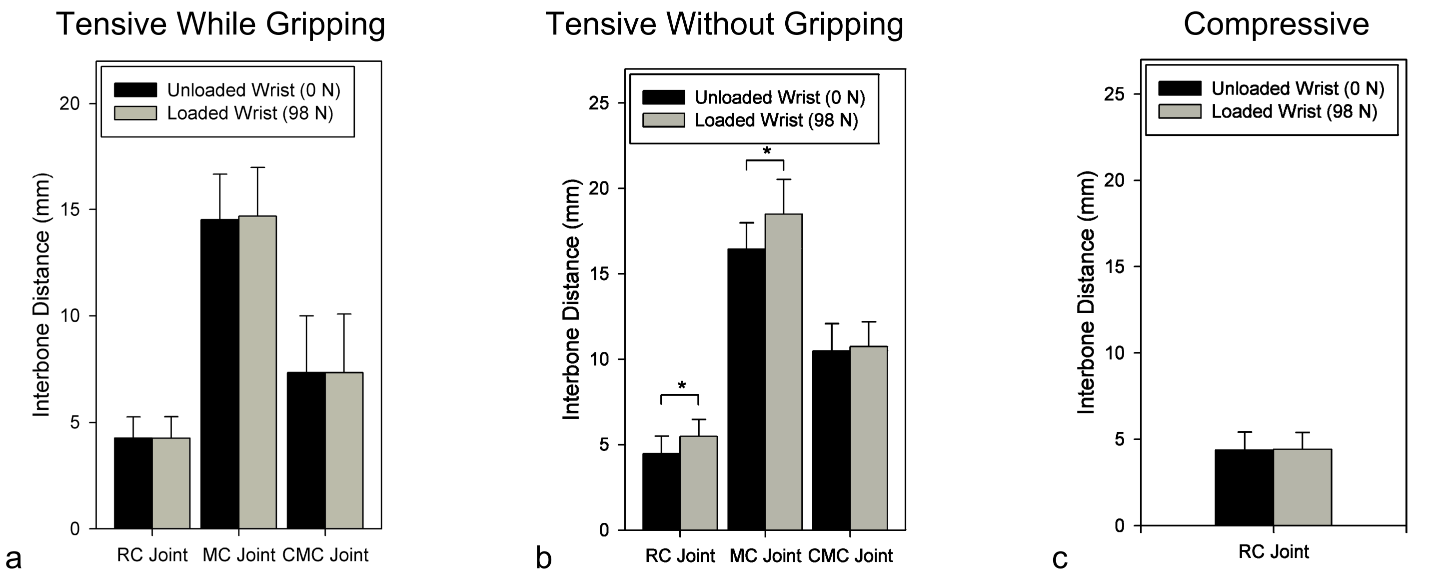

Figure F2-4. a) Tension while gripping had no affect on relative bone translation at the RC, MC, or CMC joints. b) Tension without gripping caused significant (*) bone translation at the RC and MC joint, but had no affect on the CMC joint. c) Compression had no affect on relative bone translation at the RC joint.